THE JOURNAL OF BIOLOGICAL CHEMISTRY
Vol. 271, No. 14, Issue of April 5, pp. 8115–8120, 1996

Printed in U.S.A.

The 5′-Untranslated Region of the *N*-Methyl-D-aspartate Receptor NR2A Subunit Controls Efficiency of Translation*

(Received for publication, December 4, 1995, and in revised form, January 17, 1996)

Michael W. Wood‡, Hendrika M. A. VanDongen, and Antonius M. J. VanDongen§

From the Department of Pharmacology, Duke University, Durham, North Carolina 27710

The *N*-methyl-D-aspartate (NMDA) receptor plays a central role in such phenomena as long term potentiation and excitotoxicity. This importance in defining both function and viability suggests that neurons must carefully control their expression of NMDA receptors. Whereas the NR1 subunit of the NMDA receptor is ubiquitously transcribed throughout the brain, transcription of NR2 subunits is spatially and temporally controlled. Since heteromeric assembly of both subunits is required for efficient functional expression, post-transcriptional modification of either subunit would affect NMDA receptor activity. Here it is demonstrated that the 5′-untranslated region (5′-UTR) of the NR2A subunit severely restricts its protein translation in both *Xenopus* oocytes and in an *in vitro* translation system. Mutational analysis of the 5′-UTR implicates secondary structure as the major translational impediment, while the five alternate start codons play minor roles. An important biological role for the 5′-UTR of NR2A is further suggested by the unusually high level of sequence conservation between species. In contrast, the 5′-UTR of NR1 does not inhibit translation and is not conserved. Taken together, these findings suggest a mechanism for modulation of NMDA receptor activity through the control of translational efficiency of a single subunit.

Fast synaptic excitatory neurotransmission within the central nervous system is mediated primarily by the neurotransmitter glutamate (1). Of the class of ligand gated ion channels responsive to glutamate, the NMDA receptor possesses a unique calcium permeability. This property, along with the voltage-dependent magnesium block, governs the role of the NMDA receptor in such phenomena as long term potentiation and excitotoxicity (1). NMDA receptor function is also critical for proper organization of synaptic networks during development (2). The importance of modulation of NMDA receptor activity is exemplified in models of excitotoxicity, in which unrestricted channel activity induces neurodegeneration through excessive calcium influx (3). Thus, a delicate balance between essential neuronal function and survival suggests that the quantity of functional NMDA receptors must be controlled. The initial cellular mechanism for control of protein expression resides at the level of transcription. However, translational regulation has also been proposed as a means of directing protein synthesis (4, 5).

The NR1 subunit of the NMDA receptor is ubiquitously transcribed throughout the brain. In contrast, NR2 subunits display distinct regional and developmental transcription profiles. *Xenopus laevis* oocytes injected with NR1 mRNA form functional channels with small agonist responses. Although NR2 subunits do not form functional receptors when expressed alone, they enhance function when coinjected with NR1. The importance of NR2 subunits is emphasized by the behavioral deficits that result from the targeted disruption of the NR2A gene (6). Here, using the *Xenopus* oocyte expression system, it is shown that an encumbrance within the 5′-UTR[1] of the NR2A subunit is capable of restricting its translation to 1% of the potential maximum. Thus, it is demonstrated that the 5′-UTR of a single subunit is able to control NMDA receptor activity over a range of three orders of magnitude. Furthermore, it is recognized that the 5′-UTR of the NR2A subunit is highly conserved across species. These findings suggest a conserved mechanism for translational control of NMDA receptor activity.

EXPERIMENTAL PROCEDURES

Molecular Biology—Site-directed mutagenesis, *in vitro* transcription, and oocyte expression was performed as described previously (7). Truncation mutations, mutations eliminating stem-loops, and the mutation of alternate start codon 3 utilized a single polymerase chain reaction. Mutations of alternate AUGs and rearrangement of stem 5 utilized the megaprimer polymerase chain reaction technique (8). Rearrangement of stem 5 was accomplished utilizing a primer designed to change five of the guanines and cytosines in the shaded region of Fig. 2 to cytosines and guanines, respectively (GCTGTCGCCGCGTGTCCGCATCAC). AUG 3 was mutated to UUG, AUG 4 to AUA, and AUG 5 to AUA. All mutations were confirmed by sequencing (United States Biochemical Corp.). The sequence of the full-length ϵ1 cDNA 5′-UTR was determined by first subcloning a fragment containing the 5′-UTR into the M13 vector allowing for single-stranded DNA sequencing. A polyacrylamide gel containing formamide was used to reduce compression caused by secondary structure. *In vitro* transcription was performed using T7 RNA polymerase and RNA cap structure analog, $m^7G(5')ppp(5')G$ (New England Biolabs) and other *in vitro* transcription reagents (Promega). All constructs were contained within a modified pBluescript vector (Stratagene) and shared the following vector-derived leader sequence: GAATTGGGCGGGCCCCCCCTCGAG. The full-length ϵ1 cDNA contained the following leader sequence: GAATTGGGCGGGCCCCCCTCGAGGTCGACTCTAGAGGATCC. All cDNAs were linearized with *Not*I (New England Biolabs) before run-off transcription. All cRNAs were radiolabeled using cytidine 5′-[α-^{32}P]triphosphate, quantitated by scintillation counting, and diluted to a uniform concentration of 100 ng/μl. Aliquots of the transcripts were visualized on agarose gels to confirm that they ran as single bands of equal intensity. All data represent measurements from at least two separate transcription reactions for every construct.

Electrophysiology—Oocyte injection and whole cell voltage clamp measurements were performed as described previously (7). The NR1 cDNA clone was kindly provided by Dr. Shigetada Nakanishi (9). The ϵ1

* This work was supported by Grant NS31557 from the National Institute of Neurological Disorders and Stroke (to A. M. J. V. D.). The costs of publication of this article were defrayed in part by the payment of page charges. This article must therefore be hereby marked "*advertisement*" in accordance with 18 U.S.C. Section 1734 solely to indicate this fact.

‡ Supported by National Research Service Award MH11278 from the National Institute of Mental Health.

§ To whom correspondence should be addressed. Tel.: 919-681-4862; Fax: 919-684-8922; E-mail: vando005@mc.duke.edu.

[1] The abbreviations used are: UTR, untranslated region; PAGE, polyacrylamide gel electrophoresis; ORF, open reading frame.

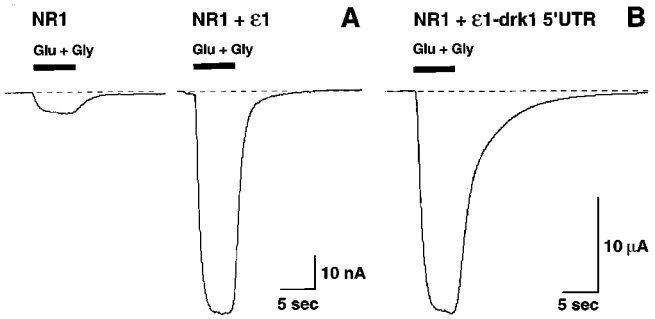

FIG. 1. **The 5′-UTR of ϵ1 (mouse NR2A) hinders translation in oocytes.** Representative current traces obtained using two-electrode voltage clamp recordings of oocytes injected with equal quantities of cRNAs encoding NR1, NR1+NR2A (ϵ1 with full-length 5′-UTR), or NR1+NR2A-drk1 5′-UTR (ϵ1 containing 5′-UTR of drk1). Coapplications of 100 μM L-glutamate and 10 μM glycine are represented by *shaded bars*. Cells were maintained at a holding potential of −50 mV. Note that scale bars represent 5 s and either 10 nanoamperes (*A*) or 10 microamperes (*B*).

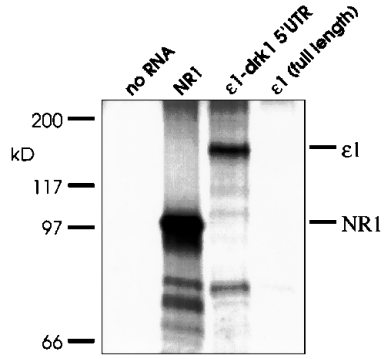

FIG. 2. **SDS-PAGE of *in vitro* translation products.** A rabbit reticulocyte lysate system was used to translate the cRNAs indicated above the lanes (nomenclature is the same as in Fig. 1). Full-length NR1 and ϵ1 containing the short 5′-UTR of drk1 translated efficiently, yielding major protein bands that ran close to their predicted molecular weights. Full-length ϵ1 translated very poorly. A faint band of the proper molecular weight was only seen after overloading the gel and overexposing the film (data not shown).

cDNA clone was a generous gift of Dr. Masayoshi Mishina (10). All measurements were made 4 days after cRNA injection at a holding potential of −50 mV. All recordings were made in a Mg^{2+}- and Ca^{2+}-free solution containing, in mM: 140 NaCl, 5 KCl, 0.5 $BaCl_2$, 10 HEPES, pH = 7.40. Peak current responses to agonist application and accompanying voltage measurements were determined using PCLAMP hardware and software (Axon Instruments, Burlingame, CA).

In Vitro Translation—In vitro translation was performed using a rabbit reticulocyte lysate system (Promega), according to manufacturer's instructions. cRNA (25 μg/reaction) was added to the reaction mixture together with [^{35}S]methionine (Amersham Corp.). The resulting protein products were separated using SDS-PAGE. Proteins were visualized along with ^{14}C-labeled protein standards (Life Technologies, Inc.) using autoradiography.

Determining Local GC Content—A moving average was used with a window size of 21 nucleotides, after assigning the value 0 to A and U residues and the value 1 to G or C residues. A weighted average was obtained by multiplying each value with a Gaussian factor, centered at nucleotide 11 and with a standard deviation of 5 nucleotides. The average was assigned to the center of the window and plotted against nucleotide number.

RESULTS

Expression of recombinant NMDA receptors in *Xenopus* oocytes has shown that the NR1 subunit can direct expression of functional homomeric channels (9). NR2 cDNA clones do not form functional channels unless coexpressed with NR1 (11). Our initial attempts to express heteromeric NMDA receptors in *Xenopus laevis* oocytes failed to produce robust agonist responses (Fig. 1). In an effort to increase the level of expression of the NR1 + ϵ1 (murine NR2A) combination, the 5′-UTR of ϵ1 was replaced with that of drk1, a K^+ channel cDNA clone known to translate well in *Xenopus* oocytes (12). The resulting agonist responses were dramatically increased over those using the ϵ1 cDNA containing the full-length 5′-UTR (Fig. 1). A similar replacement of the NR1 5′-UTR (265 nucleotides in length) with that of drk1 (13 nucleotides) produced no change in the agonist response of homomeric channels (n = 20 oocytes, $p > 0.4$).

The inhibitory role of the NR2A 5′-UTR on translation could be a unique characteristic of the *Xenopus* oocyte expression system. We therefore studied the effect of the 5′-UTR on translation efficiency in a mammalian *in vitro* expression system. Full-length NR2A cRNA translated very poorly in a reticulocyte lysate system, while replacement of the NR2A 5′-UTR with the 5′-UTR of drk1 dramatically enhanced translation (Fig. 2). Thus the inhibitory effect of the NR2A 5′-UTR is consistent in both amphibian oocytes and a mammalian cell-free system.

Since the ϵ1 cDNA nucleotide sequence present in GenBank™ (accession number D10217) did not contain information on the 5′-UTR (10), DNA sequencing of this region (282 nucleotides) was performed (Fig. 3). This revealed that more than 99% identity exists between the 5′-UTRs of the mouse ϵ1 clone and the published rat NR2A sequence (11). Table I, which compares conservation of coding regions and 5′-UTRs for NR1 and NR2A in three species (9, 13–15), illustrates the extraordinary degree of conservation among the NR2A 5′-UTRs.

The large boost in expression level caused by replacement of the long 5′-UTR of NR2A with a 13 nucleotide sequence inferred the presence of negative regulatory elements within the 282 nucleotides. The scanning hypothesis for initiation of protein translation predicts that elements upstream of the start codon for the full-length open reading frame (ORF) are responsible for inhibiting translation (5, 16). In the 5′-UTR region of the NR2A cDNA, these include five alternative start codons (AUGs) giving rise to small open reading frames (μORFs), as well as possible structural impediments to the ribosome (*i.e.* self-complementary regions). Serial truncations of the NR2A 5′-UTR were generated and expressed in *Xenopus* oocytes in order to identify regions responsible for the inefficient translation (Fig. 4). There was no significant difference between the expression level of the full-length NR2A (282 nucleotides) and the mutation truncated at nucleotide number −196. This suggested that the primary inhibitory elements existed within the final 196 nucleotides of the NR2A 5′-UTR. Maximum expression was achieved by truncation at nucleotide number −68, suggesting that these inhibitory elements lie within the 128 nucleotides intervening nucleotides −196 and −68.

In order to investigate the importance of alternate start codons for the incremental boosts found between the serial truncations, the 5′-most AUG was mutated in each of the parent constructs that preceded a boost (Fig. 5). Mutation of AUG 3 and AUG 5 (see Fig. 3) were each found to exhibit an approximate 2-fold increase in the efficiency of translation over those of their respective parent constructs, −196 and −114. To investigate the importance of context, we also generated the AUG 5 mutation within the base construct, −196. This again resulted in an approximate 2-fold increase in translational efficiency. These results suggest that less than 5% of the translational inhibition can be attributed to the presence of alternate start codons within the 5′-UTR of NR2A and that their inhibitory effects are not affected by preceding nucleotides. Finally, the small boost in translational efficiency occurring between truncation mutants −114 an −68 can be explained by the presence of AUG 5.

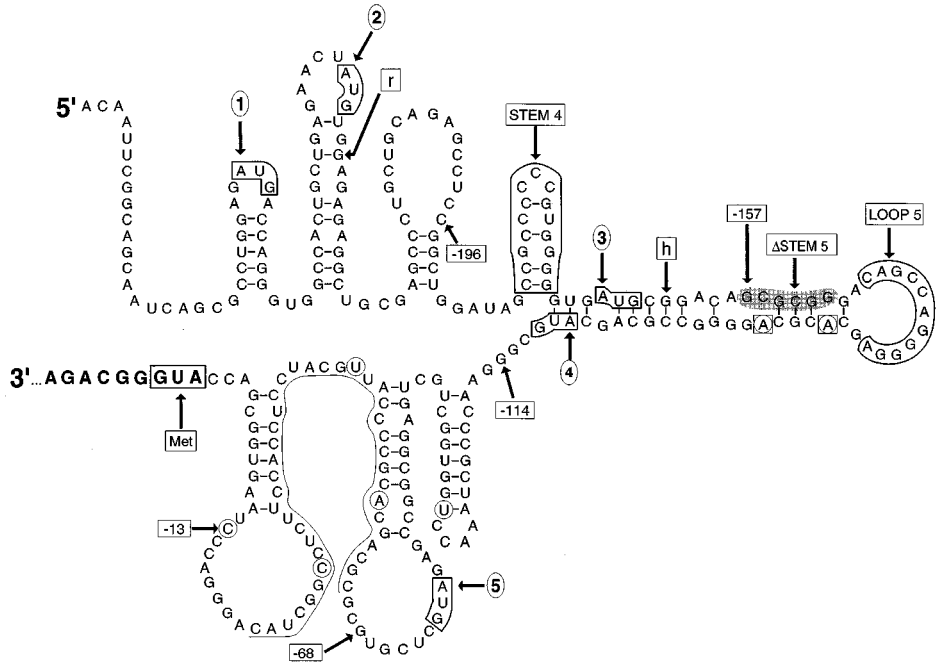

FIG. 3. **Graphical representation of the 5′-UTR of ϵ1 (mouse NR2A).** The beginning of the coding sequence for the full-length ORF is shown in *boldface*. Alternate AUGs are outlined and numbered according to their appearance in the linear sequence. Locations of the 5′-most nucleotide of each of the serial truncation mutations is indicated by the *boxed numbers*. The 5′-most nucleotide of the rat NR2A cDNA is symbolized by a *boxed r* and that of the human NR2A cDNA by a *boxed h*. The two *boxed* nucleotides mark the positions where the rat sequence is found to diverge from that of the mouse sequence, the seven *circled* nucleotides mark positions of divergence of the human sequence from that of the mouse sequence. The nucleotides outlined and labeled as *STEM 4* were replaced with the sequence 5′-TCT-3′, those of the *shaded* and labeled *STEM 5* with 5′-CGCGCC-3′. The LOOP label outlines the nucleotides deleted in the "loop" mutation of stem-loop 5. The *hairline* under nucleotides −65 through −21 illustrates the sequence exhibiting homology with the 5′-UTR of $G_{o,\alpha}$. Self-complementary structures were predicted by the StemLoop program in the Wisconsin Package of the Genetics Computer Group (Madison, WI).

TABLE I
Sequence conservation of 5′-UTR and coding regions between species

	5'UTR	Coding region
NR2A: Rat vs. Mouse	99%	95%
NR2A: Human vs. Mouse	95%	89%
NR1: Rat vs. Mouse	88%	96%
NR1: Human vs. Mouse	65%	90%

The minimal effects conferred by alternate start codons suggested an important inhibitory role for secondary structures within the NR2A 5′-UTR. Although the precise structure of the NR2A mRNA is not known, several algorithms exist which can predict possible stem-loop structures based on self-complementary regions within the 5′-UTR. One such algorithm was employed in the generation of the putative structure shown in Fig. 3. The results obtained thus far suggested that most of the translational inhibition can be localized to the nucleotides between −196 and −114. Thus, the contribution to inhibition of translational efficiency of the two putative stem-loop structures existing within this region were examined.

Removal of the nucleotides comprising the predicted loop structure of stem-loop 5 results in a 10-fold decrease in translation efficiency *versus* that of the parent construct, −157 (Fig. 6). This diminution suggests that the loop structure plays a role in relieving translational inhibition, possibly by decreasing the stability of stem 5. We then examined the role of stem-loop 5 within the context of the base construct −196. A stretch of six nucleotides within the stem was mutated such that the overall G/C content would not be diminished, yet the predicted loop structure would be expanded. No effect on translational efficiency is evident from this mutation. The final mutation of secondary structure targeted stem-loop 4. To avoid consequently placing AUG 3 into an unusual context, we generated a mutant lacking both stem-loop 4 and AUG 3. This resulted in a 40-fold increase in translation efficiency (Fig. 6).

Finally, it has been demonstrated that certain mRNAs can be translated in a cap-independent fashion (17). Therefore, the synthetic m^7G cap analog was omitted from an *in vitro* translation preparation of full-length NR2A. This resulted in a predicted reduction in the translational efficiency. Uncapped, full-length NR2A did not result in a detectable boost of expression level when coinjected with NR1 ($n = 21$, $p > 0.3$). Thus, translation of full-length NR2A is cap-dependent.

DISCUSSION

Considerable data have been generated documenting the importance of 5′-UTRs in defining the translatability of mRNAs (16–18). The longstanding ribosome scanning model has adequately predicted many of the findings, although several alternative models have arisen to explain specific aberrant cases of translational control (5, 17, 19, 20). Furthermore, of the relatively few mRNAs which posses 5′ encumbrances, most fall into several categories of proteins critically important to maintaining cellular viability (*e.g.* growth hormone receptors and proto-oncogenes) (5). A leading hypothesis suggests that translation of mRNAs containing structured 5′-UTRs might be selectively modulated through the regulation of helicases capable of relieving structural impediments (17, 20). Indeed, evidence of this mechanism involving control of specific translation initiation factors supports this hypothesis. Modulation may occur through the phosphorylation and consequent disruption of the binding properties of a protein (4E-BP1) which otherwise inhibits a critical initiation factor (eIF-4E) (4). Alternatively, the presence of extensive structural configurations may also decrease the global rate of translation through a

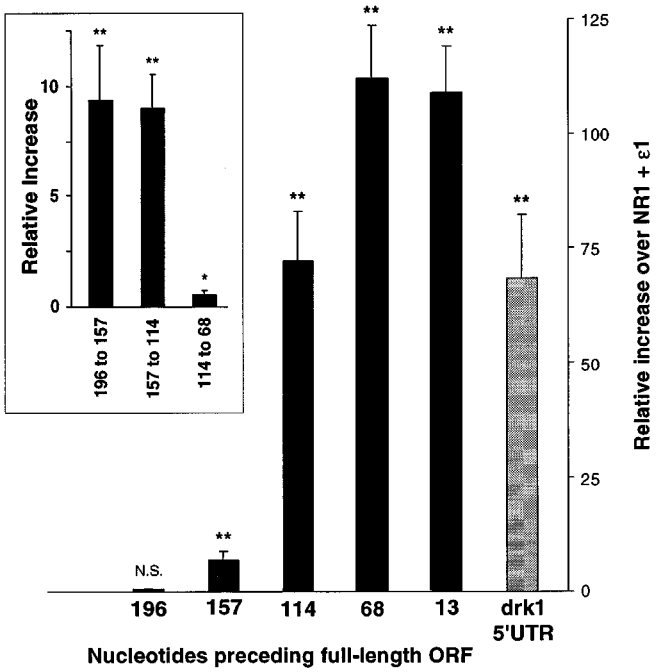

FIG. 4. **Effect of serial truncation of the 5′-UTR of NR2A (ϵ1).** Electrophysiological measurements as described in Fig. 1 were performed on oocytes injected with combinations of NR1 and each of the indicated NR2A mutants. The chart represents subsequent comparisons of the resulting measurements with measurements of oocytes injected with the NR1+ϵ1 combination containing the full-length ϵ1 5′-UTR. The *inset* shows the incremental boosts conferred by successive truncations as compared with the previous (longer) construct. *Error bars* represent standard errors of the mean (S.E.). p values of less than 0.001 are denoted by **, and $p < 0.05$ by *. *N.S.* indicates no significant change from the NR1+ϵ1 combination. Measurements were performed on at least four batches of oocytes for each construct (11 batches total) and at least five oocytes for each batch. Mean current measurements and total oocytes measured are as follows: NR1 alone, 14 ± 11 nA, n = 56; NR1+ϵ1, 143 ± 50 nA, n = 27; NR1+ϵ1–196, 99 ± 20 nA, n = 40; NR1+ϵ1–157, 1.0 ± 2.4 μA, n = 45; NR1+ϵ1–114, 10.3 ± 1.6 μA, n = 25; NR1+ϵ1–68, 15.9 ± 1.7 nA, n = 20; NR1+ϵ1–13, 15.6 ± 1.4 μA, n = 21; NR1+ϵ1-drk1 5′-UTR, 9.8 ± 2.0 μA, n = 20.

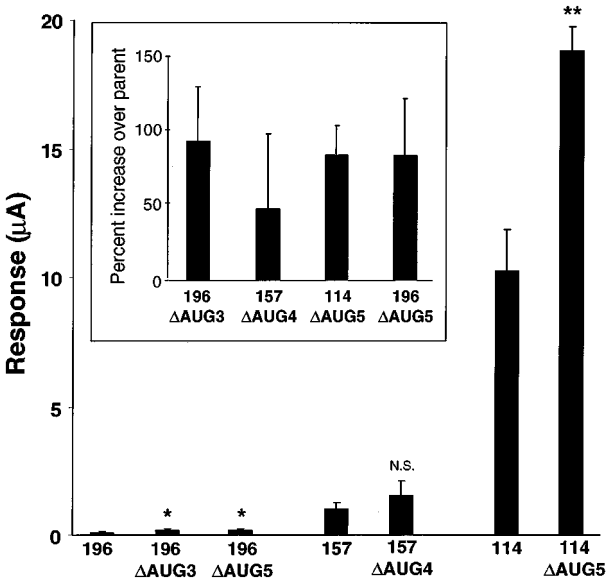

FIG. 5. **Effect of mutations of individual alternate AUGs.** Measurements of whole current responses are charted for each of the parent truncation mutants and their respective AUG mutations. *Error bars* represent S.E. values. p values of less than 0.001 are denoted by ** and $p < 0.05$ by *. The *inset* shows the comparison of AUG mutations normalized to parent constructs. Measurements were performed on at least three batches of oocytes for each construct and at least five oocytes for each batch. Mean current measurements and total oocytes measured are as follows: NR1+ϵ1–196ΔAUG3, 191 ± 33 nA, n = 20; NR1+ϵ1–196ΔAUG5, 181 ± 35 nA, n = 15; NR1+ϵ1–157ΔAUG4, 1.5 ± 0.5 μA, n = 25; NR1+ϵ1–114ΔAUG5, 18.8 ± 1.0 μA, n = 20.

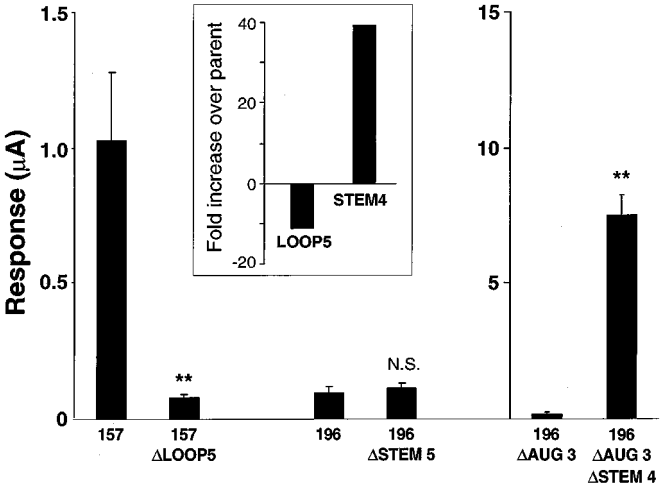

FIG. 6. **Mutations affecting putative secondary structures.** Measurements of whole current responses are charted as in Fig. 4. The *inset* shows the relative decrease from the deletion of the loop structure in stem-loop 5 and the relative increase from the deletion of stem-loop 4. *Error bars* represent S.E. values. p values of less than 0.001 are denoted by **. Measurements were performed on three batches of oocytes for each construct and five oocytes for each batch. Mean current measurements and total oocytes measured are as follows: NR1+ϵ1–157ΔLOOP, 84 ± 9 nA, n = 15; NR1+ϵ1–196ΔSTEM5, 114 ± 20 nA, n = 15; NR1+ϵ1–196ΔAUG3ΔSTEM-LOOP4, 114 ± 20 nA, n = 15.

mechanism involving a double-stranded RNA-activated protein kinase (PKR) (20). Finally, instances of translational control defined by developmental stage and tissue specificity have also been documented (18, 21).

The NR1 subunit is essential for expression of functional NMDA receptors (9). However, electrophysiological measurements demonstrate that homomeric NR1 channels express quite poorly in *Xenopus* oocytes and that apparently these channels are functionally undetectable in mammalian heterologous expression systems. Indeed, here we show that for *Xenopus* oocytes, functional activity of homomeric NR1 receptors is only 0.1% of that of heteromeric receptors utilizing efficiently translating NR2A subunits (Fig. 1). Therefore, efficient functional expression requires both NR1 and NR2 subunits.

In vitro translation of the full-length ϵ1 cRNA using a rabbit reticulocyte lysate system mimicked the results found in *Xenopus* oocytes (Fig. 2). Apparent molecular weights predicted to arise from initiation at alternate AUGs 1 through 5 are 3.5, 11.9, 2.1, 1.1, and 7.0 kilodaltons, respectively. The spurious band seen on the SDS-PAGE gel at approximately 75 kilodaltons may represent either premature termination or degradation of the ϵ1 protein. Thus, no peptide products from the alternate μORFs were evident. This finding is consistent with previous reports suggesting that these AUGs may only temporarily "stall" the scanning ribosome (5). The consistency of findings between the two systems argues that the analysis performed on translational inhibition in oocytes is representative of the inhibitory mechanisms of mammalian cells. Furthermore, because this analysis involves RNA that is transcribed *in vitro* and microinjected into the oocyte cytoplasm, the inhibition would not be expected to involve the oocyte mRNA masking phenomenon (22).

No cell-specific transcriptional control over the NR1 gene is apparent beyond that of alternative splicing and restriction to the central nervous system (23). In contrast, the NR2 subunits

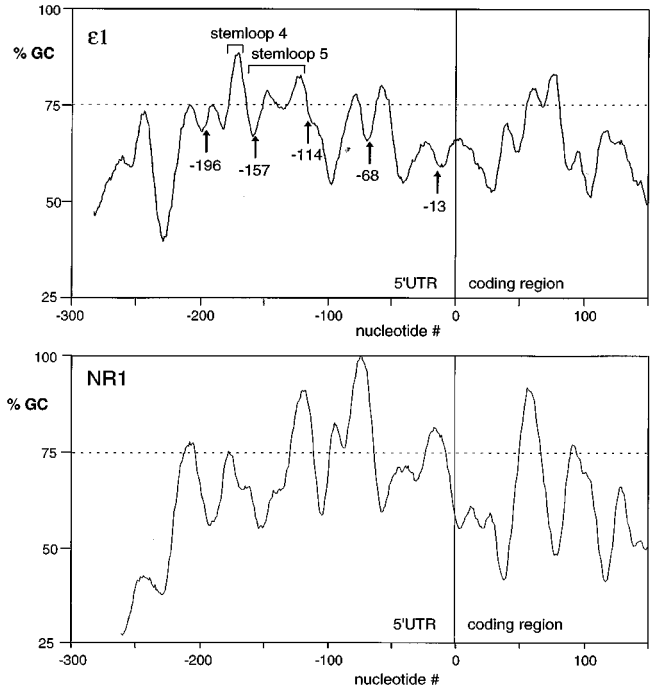

FIG. 7. **Profiles of GC content for 5′-UTRs of ϵ1 and NR1.** Local GC content of the 5′-UTR was estimated as described under "Experimental Procedures" for both ϵ1 and NR1. The positions of the different truncations as well as putative stem-loops 4 and 5 are indicated. GC content per se does not seem to explain the difference in translatability between the two NMDA receptor subunits. The overall GC content of the 5′-UTR is 67% for both NR1 and ϵ1. Also, NR1 has a local maximum which is higher and more extensive than the maximum at stem-loop 4 in ϵ1.

are regulated according to developmental stages and cell types (24, 25). While functional NMDA receptors require the constitutively expressed NR1 subunit, the results presented here infer that the biological relevance of these receptors is regulated by the controlled expression of the NR2 subunits. Furthermore, our results suggest that some of this regulation may be imparted by control of translational efficiency.

This study demonstrates that the translational control mechanism is present only in the 5′-UTR of the NR2 subunit and not in the 5′-UTR of the NR1 subunit. The difference in translatability of the two messages does not arise from any general features of the 5′-UTRs. The 5′-UTRs of both subunits possess similar nucleotide lengths, identical overall G/C content and comparable GC profiles (Fig. 7). Emphasis of the contrast is rendered by the sequence homology comparisons shown in Table I. Homology comparisons of the coding sequences demonstrate that both subunits exhibit a similar degree of conservation (approximately 95% *versus* rat and 90% *versus* human). However, within the 5′-UTRs of the two subunits, relatively little conservation is seen for the NR1 subunit in comparison with the very high degree of conservation for the NR2 subunit. The relative level of sequence homology alone argues for a pertinent role for the 5′-UTR of the NR2A subunit.

The gene sequence for the murine NR2C subunit has been determined (26). The fact that this NR2 subunit is alternatively spliced only within its 772 nucleotide long 5′-UTR again is suggestive of a role in translational regulation. No gene sequence is available for the NR2A subunit. However, a Northern blot of the NR2A subunit displays a major band of approximately 18 kilobases (10). If this huge message represents unspliced pre-mRNA, then this would suggest the application of another post-transcriptional regulatory mechanism (*i.e.* via controlled splicing). This has been previously reported for other

TABLE II

Comparison of contexts of alternate and coding AUGs

Nucleotides surrounding the alternate start codons in the 5′-UTR of ε1 (μORFs 1–5) as well as the assigned start codons for ε1 (ORF) and dkr1 are compared with the "ideal" context as described by Kozak (5). The right-most column lists the number of matches.

position	-6	-5	-4	-3	-2	-1	1	2	3	4	
Kozak	**G**	**C**	**C**	**A/G**	**C**	**C**	**A**	**T**	**G**	**G**	7
μORF #1	C	T	G	G	A	G	A	T	G	A	1
μORF #2	A	G	A	A	C	T	A	T	G	T	2
μORF #3	G	G	G	G	T	G	A	T	G	C	2
μORF #4	C	G	C	A	G	C	A	T	G	C	3
μORF #5	G	C	C	G	A	G	A	T	G	C	4
ORF	G	C	G	A	C	C	A	T	G	G	6
drk1	T	C	T	G	G	C	A	T	G	G	4

messages (5). We cannot rule out the possibility that a significant portion of the endogenous 5′-UTR remains unrepresented in the cDNA clone. The addition of upstream nucleotides may relieve impediments found within the 5′-UTR of the NR2A cRNA, although our results provide no support for this hypothesis.

Our results do suggest that control of translational efficiency is largely derived from the 128 nucleotides found between nucleotide numbers −196 and −68. Little of the inhibition appears to arise from the five alternate start codons found within the 5′-UTR. Table II compares the sequences surrounding the coding and alternate AUGs with the Kozak consensus sequence. The alternate AUGs show a less favorable context than the coding AUGs. In particular, they are missing the important G at position +4. The surrounding nucleotide sequence is important for the AUG of the full-length ORF. A near-perfect sequence is present in the mutant truncated at nucleotide number −13. This truncation mutation translates more efficiently than the construct containing the 5′-UTR of drk1 ($p < 0.001$, Fig. 4), which possess identical length and less consensus integrity.

The relatively small impact of the alternate start codons implies that the dominant effect is due to secondary structure. A structural model of the 5′-UTR was generated in order to facilitate the planning of experiments testing the relative effects of secondary structure on translational inhibition. During the construction of this model, several interesting regions of sequence homology were recognized. Of minor notation is the observation that 10 of 12 nucleotides within the loop of proposed stem-loop structure 5 display homology with the loop of the *trans*-acting responsive (TAR) element structure of human immunodeficiency virus-1 (27). Although loop 5 possesses 70% G/C content, its deletion identified it as a positive regulator of translational efficiency. However, rearranging several nucleotides found within the stem portion of stem-loop 5 in an attempt to expand this putative loop structure did not provide further relief of translational inhibition. This result may be due to a rematching of the scrambled nucleotides into a new stem-loop configuration.

In contrast, the elimination of stem-loop structure 4 (93% G/C content) provided considerable relief of inhibition, clearly substantiating its role as a negative regulator of translation. The relief provided by the elimination of stem-loop 4 was greater than what would be expected based on the results of the truncation mutations. This is likely due to the induction of a novel folding structure of the mRNA. Alternatively, the elimination of stem-loop 4 may have added an increment of unmatched nucleotides between the 5′-cap and downstream self-

complementary structures. This addition may have permitted ample initiation access for the ribosome to unwind downstream secondary structures of lesser stability as has been reported previously (5). Another alternative explanation for these findings which has not yet been considered is the possible role of mRNA-binding proteins. It can be argued that specific sequences within the 5′-UTR may be capable of recruiting endogenous molecules which can act to stimulate or inhibit translation (18). This study provides no evidence to either substantiate or refute this hypothesis.

A more significant region of homology was recognized between the 5′-UTRs of NR2A and the α-subunit of the heterotrimeric G-protein, G_o. These 38 nucleotides are 76% identical and include an uninterrupted stretch of 15 shared nucleotides. Evidence of translational regulation of $G_{o,\alpha}$ has also been reported, as well as a high degree of sequence conservation within the 5′-UTRs across species (28). Finally, the intramolecular location of these homologous regions are downstream of the regions identified as inhibitory to translation of both mRNAs, hinting that these sequences may play similar roles in both messages.

Although there is no *in vivo* study correlating quantities of mRNA with protein levels of NMDA receptor subunits, several observations are suggestive of post-transcriptional control mechanisms. In a temporal study utilizing primary cultures of cortical neurons, an increase in NMDA receptor density as measured by antagonist binding is not accompanied by a change in mRNA levels (29). Similarly, the observation of an NMDA receptor subtype-specific increase in binding density in response to kindling of adult male rats does not arise from quantitative alterations in subunit transcripts (30). Although increases in binding density can be explained by other post-transcriptional alterations, these dichotomies of apparent protein and mRNA levels could emanate from a selective translational control mechanism.

mRNA, polyribosomes, and smooth endoplasmic reticulum (35) have been localized to dendritic processes (31, 32). Therefore, it has been speculated that synaptic activity may influence translational efficiency (33). Because the cellular organelles necessary for the assembly of integral membrane proteins (*i.e.* rough endoplasmic reticulum and Golgi apparatus) have not been observed at post-synaptic densities, this model has been restricted to include only cytoplasmic proteins. However, it is interesting to note that glutamate receptor subunit mRNAs have also been identified in neuronal processes (34).

This study has recognized that the 5′-UTR of the NMDA receptor NR2A subunit is capable of modulating the activity of this critical protein complex over 3 orders of magnitude. Little of the inhibition conferred by the 5′-UTR involves its five alternate AUGs. A large translational impediment is localized to a G/C-rich stretch of 15 nucleotides. The presence of another stretch of 11 nucleotides is recognized as a positive modulator of translation. The extraordinary sequence conservation of these untranslated nucleotides argues for an endogenous role for this sequence. Finally, recent advances make it possible to surmise that this highly conserved, strongly inhibitive sequence may represent a neuronal mechanism for regulation of NMDA receptor activity through the manipulation of translational efficiency.

REFERENCES

1. Hollmann, M., and Heinemann, S. (1994) *Annu. Rev. Neurosci.* **17,** 31–108
2. Rabacchi, S., Bailly, Y., Delhaye-Bouchaud, N., and Mariani, J. (1992) *Science* **256,** 1823–1825
3. Choi, D. W. (1988) *Neuron* **1,** 623–634
4. Pause, A., Belsham, G. J., Gingras, A. C., Donze, O., Lin, T. A., Lawrence, J. C., Jr., and Sonenberg, N. (1994) *Nature* **371,** 762–767
5. Kozak, M. (1991) *J. Cell Biol.* **115,** 887–903
6. Sakimura, K., Kutsuwada, T., Ito, I., Manabe, T., Takayama, C., Kushiya, E., Yagi, T., Aizawa, S., Inoue, Y., Sugiyama, H., and Mishina, M. (1995) *Nature* **373,** 151–155
7. Wood, M. W., VanDongen, H. M. A., and VanDongen, A. M. J. (1995) *Proc. Natl. Acad. Sci. U. S. A.* **92,** 4882–4886
8. Sarkar, G., and Sommer, S. S. (1990) *BioTechniques* **8,** 404–407
9. Moriyoshi, K., Masu, M., Ishii, T., Shigemoto, R., Mizuno, N., and Nakanishi, S. (1991) *Nature* **354,** 31–37
10. Meguro, H., Mori, H., Araki, K., Kushiya, E., Kutsuwada, T., Yamazaki, M., Kumanishi, T., Arakawa, M., Sakimura, K., and Mishina, M. (1992) *Nature* **357,** 70–74
11. Monyer, H., Sprengel, R., Schoepfer, R., Herb, A., Higuchi, M., Lomell, H., Burnashev, N., Sakmann, B., and Seeburg, P. (1992) *Science* **256,** 1217–1221
12. Frech, G. C., VanDongen, A. M. J., Schuster, G., Brown, A. M., and Joho, R. H. (1989) *Nature* **340,** 642–645
13. Karp, S. J., Masu, M., Eki, T., Ozawa, K., and Nakanishi, S. (1993) *J. Biol. Chem.* **268,** 3728–3733
14. Yamazaki, M., Mori, H., Araki, K., Mori, K. J., and Mishina, M. (1992) *FEBS Lett.* **300,** 39–45
15. Le Bourdelles, B., Wafford, K. A., Kemp, G., Marshall, C. B., Wilcox, A. S., Sikela, J. M., and Whiting, P. J. (1994) *J. Neurochem.* **62,** 2091–2098
16. Kozak, M. (1991) *J. Biol. Chem.* **266,** 19867–19870
17. Sonenberg, N. (1993) *Gene Exp.* **3,** 317–323
18. Curtis, D., Lehmann, R., and Zamore, P. D. (1995) *Cell* **81,** 171–178
19. Theil, E. C. (1993) *Biofactors* **4,** 87–93
20. Proud, C. G. (1995) *Trends Biochem. Sci.* **20,** 241–246
21. Imataka, H., Nakayama, K., Yasumoto, K., Mizuno, A., Fujii-Kuriyama, Y., and Hayami, M. (1994) *J. Biol. Chem.* **269,** 20668–20673
22. Bouvet, P., and Wolffe, A. P. (1994) *Cell* **77,** 931–941
23. Bai, G., and Kusiak, J. W. (1995) *J. Biol. Chem.* **270,** 7737–7744
24. Monyer, H., Burnashev, N., Laurie, D. J., Sakmann, B., and Seeburg, P. H. (1994) *Neuron* **12,** 529–540
25. Sheng, M., Cummings, J., Roldan, L. A., Jan, Y. N., and Jan, L. Y. (1994) *Nature* **368,** 144–147
26. Suchanek, B., Seeburg, P. H., and Sprengel, R. (1995) *J. Biol. Chem.* **270,** 41–44
27. Puglisi, J. D., Tan, R., Calnan, B. J., Frankel, A. D., and Williamson, J. R. (1992) *Science* **257,** 76–80
28. Li, Y., Mortensen, R., and Neer, E. J. (1994) *J. Biol. Chem.* **269,** 27589–27594
29. Zhong, J., Russell, S. I., Pritchett, D. B., Molinoff, P. B., and Williams, K. (1994) *Mol. Pharm.* **45,** 846–853
30. Kraus, J. E., Yeh, G.-C., Bonhaus, D. W., Nadler, J. V., and McNamara, J. O. (1994) *J. Neurosci.* **14,** 4196–4205
31. Steward, O., and Banker, G. A. (1992) *Trends Neurosci.* **15,** 180–186
32. Martone, M. E., Zhang, Y., Simpliciano, V. M., Carragher, B. O., and Ellisman, M. H. (1993) *J. Neurosci.* **13,** 4636–4646
33. St. Johnston, D. (1995) *Cell* **81,** 161–170
34. Miyashiro, K., Dichter, M., and Eberwine, J. (1994) *Proc. Natl. Acad. Sci. U. S. A.* **91,** 10800–10804
35. Harris, K. M., and Spaceck, J. (1995) *Soc. Neurosci. Abstr.* **21,** 594